



Title	Time-resolved spectroscopy studies of the photodeprotection reactions of p-hydroxyphenacyl ester phototrigger compounds
Author(s)	Ma, C; Kwok, WM; Chan, WS; Du, Y; Zuo, P; Wai Kan, JT; Toy, PH; Phillips, DL
Citation	Current Science, 2009, v. 97 n. 2, p. 202-209
Issued Date	2009
URL	http://hdl.handle.net/10722/168397
Rights	Creative Commons: Attribution 3.0 Hong Kong License

Time-resolved spectroscopy studies of the photodeprotection reactions of *p*-hydroxyphenacyl ester phototrigger compounds

Chensheng Ma, Wai Ming Kwok, Wing Sum Chan, Yong Du, Peng Zuo, Jovi Tze Wai Kan, Patrick H. Toy and David Lee Phillips*

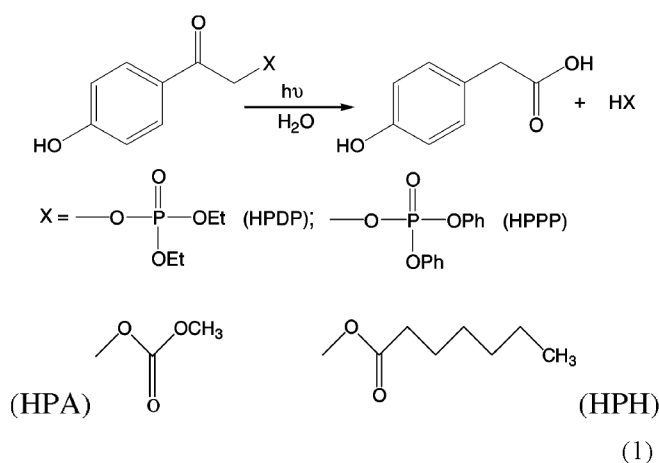
Department of Chemistry, The University of Hong Kong, Pokfulam Road, Hong Kong S.A.R., People's Republic of China

Ultrafast time-resolved spectroscopy and time-resolved resonance Raman spectroscopy experimental results in the picosecond timescales are reported for selected *p*-hydroxyphenacyl (*p*HP) ester phototrigger compounds. The results better elucidate the photodeprotection and rearrangement reactions of these important phototriggers and an overall mechanism is proposed for these reactions based on the time-resolved spectroscopy data presented here. This work indicates that site-specific, concerted solvation of the hydroxy proton and phosphate-leaving anion group through their respective intermolecular H-bonding with solvent water molecules promotes the photodeprotection reaction.

Keywords: Phototriggers, *p*-hydroxyphenacyl cage, time-resolved resonance, Raman spectroscopy, ultrafast spectroscopy.

Introduction

THERE is great interest existing in designing and developing efficient phototriggers that can be employed for real-time monitoring of physiological responses in biological systems^{1–5} and the *p*-hydroxyphenacyl (*p*HP) protecting group has been of particular interest since it has shown practical potential as a rapid and efficient ‘cage’ for the release of various biological effectors^{6,7}. Previous work has shown the photodeprotection reaction of *p*HP caged compounds takes place only in aqueous or aqueous containing solutions and does not take place in neat organic solvents like acetonitrile (MeCN)^{6,8,9}. In aqueous or aqueous containing solvents, in addition to the photodeprotection reaction, photolysis also gives rise to a photosolvolytic rearrangement of the *p*HP cage into a *p*-hydroxyphenylacetic acid (HPAA) final product (eq. (1)):



Even though the products and conditions for *p*HP deprotection have been determined in previous studies, the reaction mechanism is not well understood and most of the work utilized time-resolved transient absorption in the nanosecond to microsecond timescales in conjunction with product analysis study^{8–10}. There remains some uncertainty about the events and reactive intermediates involved in the photochemical pathway for the deprotection of *p*HP phototriggers. In this brief review, we present experimental results from a combination of ultrafast time-resolved spectroscopy and time-resolved resonance Raman spectroscopy on the picosecond and nanosecond timescales, to better elucidate the photodeprotection reaction of these important phototriggers. This work presents the first time-resolved resonance Raman (TR³) spectroscopic investigation of these types of phototrigger compounds. TR³ spectroscopy is a powerful tool to gain structural information and to explicitly identify electronic excited states and chemical reactive intermediates. The results shown here help us to better understand the overall mechanistic details of the *p*HP photochemistry and allow us to resolve the apparent controversy about the relevant reactive intermediate(s) involved in the deprotection and rearrangement pathways of *p*HP caged phototrigger compounds examined in previous work by other groups^{6,8,9}.

*For correspondence. (e-mail: phillips@hkuc.hku.hk)

Experimental methods

The *p*-hydroxyphenacyl acetate (HPA), *p*-hydroxyphenacyl diethylphosphate (HPDP) and *p*-hydroxyphenacyl diphenylphosphate (HPPP) phototriggers were synthesized following the methods given in the references 11–12 and the identity and purity of these compounds were confirmed by analysis of MS, NMR and UV absorption spectroscopy. HPAA is commercially available and was utilized after recrystallization. Spectroscopic-grade MeCN, CF₃CH₂OH and DMSO as well as deionized water were employed as solvents for the experiments discussed here.

The femtosecond transient absorption (fs-TA), Kerr-gated time-resolved fluorescence (fs-KTRF) and ps-TR³ experiments were all done using a commercial Ti:sapphire regenerative amplifier laser system equipped with a home-made OPA system that provides a tunable femtosecond/picosecond light source^{11,12}. The temporal difference between the pump (267 nm) and probe pulses used in the various femtosecond/picosecond spectroscopy experiments were controlled using an optical delay line. The time resolution of the fs-TA and fs-KTRF measurements was about 150–200 fs and sample solutions of ~1 mM concentration were used in these experiments. fs-TA experiments were done for HPDP and HPPP in neat MeCN and H₂O/MeCN (1 : 1 by volume) mixed solvents and also in typical solvents, viz. DMSO, CF₃CH₂OH and the mixture of these two, in order to examine specific solvent effects. For the ps-TR³ measurements, the samples were pumped with the 267 nm laser pulse and a probe laser pulse of either 200, 342 or 400 nm wavelength (depending on the species or process being studied) was used to generate the resonance Raman spectra. The pump and probe pulse durations were ~1.5 ps and the time-resolution of the ps-TR³ experiments was around 2–3 ps. Sample concentration of ~1–1.5 mM was used with the pump and probe beams loosely focused onto the thin stream of the sample solution. Nanosecond time-resolved resonance Raman experiment (ns-TR³) measurements with 267 nm pump and 416 nm probe laser pulses were also done for some phototriggers. The Raman light was collected in a backscattering configuration and detected by a liquid nitrogen-cooled CCD detector. Each TR³ spectrum shown here was obtained by accumulating over 2 min with an appropriately scaled pump-only and probe-only spectra being subtracted from a pump-probe spectrum, and acetonitrile Raman bands were used to calibrate the TR³ spectrum with an estimated accuracy of ± 5 cm⁻¹ in absolute frequency. Details of the experimental apparatus and methods employed for our ns- and ps-TR³ experiments are available in the literature^{11–15}.

Results

Figure 1 *a* shows the 3D contour of the KTRF spectra for HPA obtained with 267 nm excitation in MeCN, with a time delay up to 4 ps after excitation. The fluorescence

profile displays an intense emission band with a maximum near 340 nm predominates at very early times that disappears at ~0.5 ps and evolves into a relatively weak emission band that has a maximum ~420 nm and persists up to ~3 ps. The fluorescence decay kinetics at 330 and 440 nm and the instrument response function (IRF) are displayed in Figure 1 *b*. By convolution with the IRF, both the decay curves can be simulated satisfactorily by a

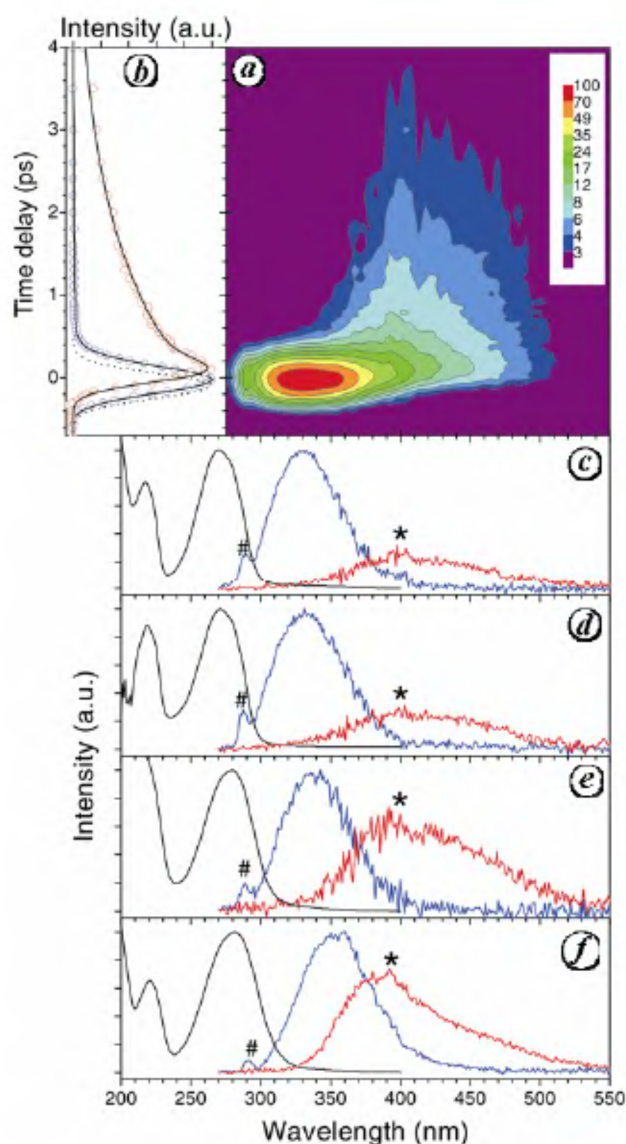


Figure 1. *a*, fs-KTRF contour of HPA obtained with 267 nm excitation in MeCN. *b*, Normalized fluorescence decay at 330 nm (circles in blue) and 440 nm (circles in red) for HPA in MeCN. The solid lines show two exponential fittings to the experimental data, and the dotted line is the instrumental response function (see reference 11 for details). *c–f*, Steady-state absorption spectrum (in black) and typical fluorescence profile of the blue (in blue) and red (in red) fluorescence for HPA in MeCN (*c*), THF (*d*), MeOH (*e*) and 90% H₂O/10% MeCN mixed solvent (*f*). The absorption spectra were normalized to the blue fluorescence spectra. Sharp features indicated by ‘#’ and ‘*’ are the solvent Raman band and the second harmonic generation of the 800 nm gating pulse from the Kerr medium respectively. (Reprinted with permission from reference 11. Copyright (2005) American Chemical Society.)

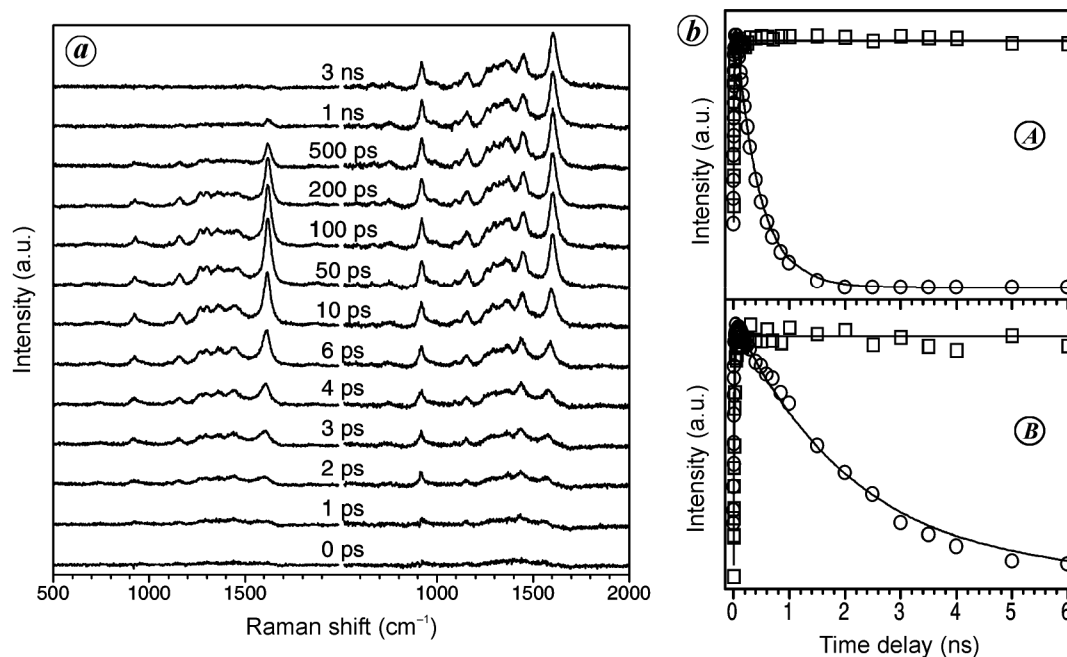


Figure 2. *a*, Picosecond Kerr-gated time-resolved resonance Raman spectra of HPDP obtained with 267 nm pump and 400 nm probe wavelengths in 50% H₂O/50% MeCN mixed solvent (left) and neat MeCN (right). *b*, Temporal dependence of the triplet ~ 1600 cm⁻¹ band areas for HPDP (*A*) and HPA (*B*) in 50% H₂O/50% MeCN mixed solvent (circles) and neat MeCN (squares) obtained in 400 nm probe ps-KTR³ spectra. Solid lines show an exponential fitting of the experimental data. (Reprinted with permission from ref. 11. Copyright (2005) American Chemical Society.)

sum of two exponential components with time constants of 0.08 and 1.78 ps respectively, but using different proportionality factors. The decay kinetics at other wavelengths can be fitted in the same manner and we take the spectra at -0.2 and 0.9 ps (displayed in Figure 1 *c*) to be representative of the net fluorescence spectrum for the short-lived blue and longer-lived red emissive excited states. The *p*HP moiety is the chromophore associated with the 267 nm photoexcitation of these compounds that leads to the prompt population of the strongly allowed $\pi\pi^*$ (L_a type) S_3 state associated with the lowest strong absorption band (shown in Figure 1 *c*). Extensive studies on aromatic carbonyl compounds show that the energy levels of the excited $\pi\pi^*$ and $n\pi^*$ states are affected significantly so that increasing the H-bonding strength or polarity stabilizes the $\pi\pi^*$ states, whereas these effects destabilize the $n\pi^*$ state at the same time. This solvent-dependent energy-level changes account for the characteristic blue shift of the $n\pi^*$ and red shift of the $\pi\pi^*$ spectral bands in solution^{16–18}. KTRF measurement in solvents of different polarity and H-bonding ability helps assign the observed fluorescence. Inspection of Figure 1 *c–f* shows that from MeCN to MeOH to H₂O/MeCN mixed solvent, the blue fluorescence downshifts to the red and the red fluorescence upshifts to the blue. This indicates the coexistence of two fluorescence components; one is the $\pi\pi^*$ character state emitting the blue fluorescence and the other is the $n\pi^*$ state emitting the red fluorescence. The results here present the first ultrafast time-resolved

fluorescence study on the *p*HP phototrigger compounds and also for related aromatic carbonyl compounds.

Figure 2 *a* displays the comparison between the ps-TR³ spectra obtained in 50% H₂O/50% MeCN (v : v) mixed solvent and those obtained in neat MeCN for HPDP. The 400 nm probe wavelength is near the maximum position of the $T_1 \rightarrow T_n$ absorption band⁹. The similarity between the spectra in the two solvents indicates that the spectra in the H₂O/MeCN mixed solvent can be confidently attributed to the HPDP $^3\pi\pi^*$ state. In Figure 2 *b*, (*A*) and (*B*) shows kinetic comparisons for the $^3\pi\pi^*$ states in pure MeCN and H₂O/MeCN mixed solvent for HPDP and HPA respectively. The early time $^3\pi\pi^*$ development is similar for both the compounds in the two solvents (with ~ 7 – 12 ps time constants for the triplet growth), but the $^3\pi\pi^*$ lifetime is much shorter in H₂O/MeCN mixed solvent than in pure MeCN solvent. This solvent and leaving group-dependent quenching of the triplet implies that further reaction(s) takes place on the triplet manifold, specifically in the H₂O-containing solvent. Figure 3 *a* shows early time ps-KTR³ spectra in the 1450 – 1800 cm⁻¹ region for HPDP in 50% H₂O/50% MeCN mixed solvent using 400 and 342 nm probe wavelengths after 267 nm pump excitation. The band at ~ 1610 cm⁻¹ appearing at 2 ps and afterwards at both probe wavelengths is from the same $^3\pi\pi^*$ triplet also seen in spectra acquired in neat MeCN solvent (Figure 2). Figure 3 has an additional Raman band at about 1550 cm⁻¹, only seen at very early times (up to 4 ps) and this band decays very fast to form

the $^3\pi\pi^*$ triplet state and the absence of the early time $\sim 1550\text{ cm}^{-1}$ Raman band in the 400 nm probe ps-TR³ spectra implies that this band is from another short-lived species that is not the $^3\pi\pi^*$ triplet state. The $\sim 1550\text{ cm}^{-1}$ Raman band correlates with the lifetime of the red fluorescence of the $^1n\pi^*$ S_1 state seen in the preceding KTRF spectra, and we assign the new early time $\sim 1550\text{ cm}^{-1}$ Raman band to be due to the $^1n\pi^*$ S_1 state. Our result that the intersystem crossing (ISC) occurs from the $^1n\pi^*$ S_1 state even with S_3 excitation implies that the major deactivation channel of the photo-populated S_3 state is internal conversion to S_1 .

In Figure 3, the temporal growth of the triplet band intensity is accompanied by slight frequency upshift (by $\sim 40\text{ cm}^{-1}$) and bandwidth narrowing (by $\sim 40\text{ cm}^{-1}$) for HPA and HPDP in both H₂O/MeCN mixed and neat MeCN solvents (for details of these changes in spectral profile, the reader is referred to references 19 and 20). Such an early time spectral change in Raman band profile is a characteristic indication of an excess energy relaxation process^{19,20} that has a typical timescale of around 10 ps, which agrees well with the ~ 7 –12 ps time constant observed here. The observed early stage $^3\pi\pi^*$ spectral evolution is assigned to combined dynamics involving growth of the triplet population and subsequent relaxation of excess energy ($\sim 11,000\text{ cm}^{-1}$) introduced by 267 nm excitation and rapid ISC conversion.

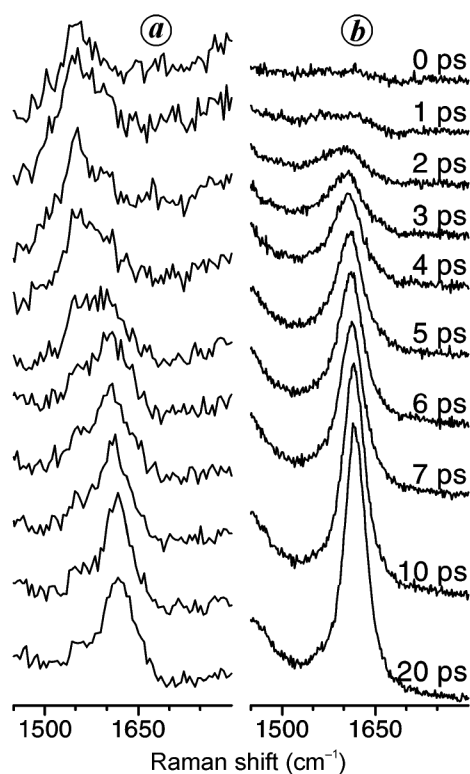


Figure 3. Picosecond Kerr-gated time-resolved resonance Raman spectra obtained for HPDP in 50% H₂O/50% MeCN mixed solvent with 267 nm pump and 342 nm probe (a) and 400 nm probe (b) wavelengths respectively. (Reprinted with permission from ref. 11. Copyright (2005) American Chemical Society.)

Figure 4a shows the fs-TA spectra HPDP at early (A, from 0.1 to 12 ps) and late (B, from 12 to 2000 ps) picosecond times recorded with 267 nm excitation in H₂O/MeCN (1 : 1) mixed solvent. The right-hand part in Figure 4a (A) shows profile change of the transient absorption spectra recorded over 4–12 ps. Figure 4a shows that two absorption bands (a strong one around 400 nm and a broad and weak one at 470–620 nm) grow rapidly at the expense of the middle strong band at $\sim 320\text{ nm}$ and an isobestic point at $\sim 330\text{ nm}$ indicates a dynamical conversion between two distinct states. This spectral transformation is due to the ISC conversion from the lowest singlet (S_1) to triplet (T_1), and the very early time spectra (such as the 0.25 and 0.1 ps spectra in Figure 4a (A)) should be assigned to a $S_1 \rightarrow S_n$ absorption from the $S_1(n\pi^*)$ singlet state and the fully developed spectra (12 ps spectra in Figure 4a) should be assigned to the $T_1 \rightarrow T_n$ absorption from the T_1 triplet ($\pi\pi^*$) state. Figure 4b shows fs-TA spectra kinetics of the decay of the T_1 triplet ($\pi\pi^*$) state under varying water concentrations in the mixed solvents and in some other solvent systems. A Stern–Volmer analysis based on the above triplet decay measurements in the varying water concentration mixed solvents leads to a curved and roughly quadratic dependence on water concentration and indicates that two or more water molecules are involved in the deprotection reaction. Water can act simultaneously as a HBD (hydrogen bond donor) and HBA (hydrogen bond acceptor) solvent. fs-TA measurements were also done for 267 nm photolysis of HPDP in solvents of DMSO, CF₃CH₂OH and mixed solvent of DMSO/CF₃CH₂OH (1 : 1 by volume). DMSO is a typical HBA solvent with nearly zero ability to be a HBD solvent, while CF₃CH₂OH is a good HBD solvent that is not able to act as a good HBA solvent²¹. This enables selective H-bonding with the HPDP triplet at the acidic site (phenolic proton) in the DMSO solution, at the basic site(s) (the carbonyl oxygen and phosphate anion as leaving group) in the CF₃CH₂OH solution, and at both the acidic and basic sites by the respective components in the DMSO/CF₃CH₂OH (1 : 1) mixed solvent. The TA experiment in DMSO exhibits no triplet quenching and the triplet decay kinetics is the same as that found in MeCN. A small degree of triplet quenching was observed in CF₃CH₂OH solvent but a much larger quenching was found in the DMSO/CF₃CH₂OH (1 : 1) mixed solvent. This indicates that the triplet can be quenched rather efficiently in the DMSO/CF₃CH₂OH mixed solvent, but not so much in the respective neat solvent. This suggests that the presence of solvent with both hydrogen bond donating and accepting capacities is essential for the triplet quenching step and implies further that concerted solvation at both the acidic and basic sites is needed for the deprotection reaction.

The double-bonded oxygen of the phosphate-leaving group and the hydrogen atom of the hydroxy moiety are likely the basic and acidic sites respectively, involved in

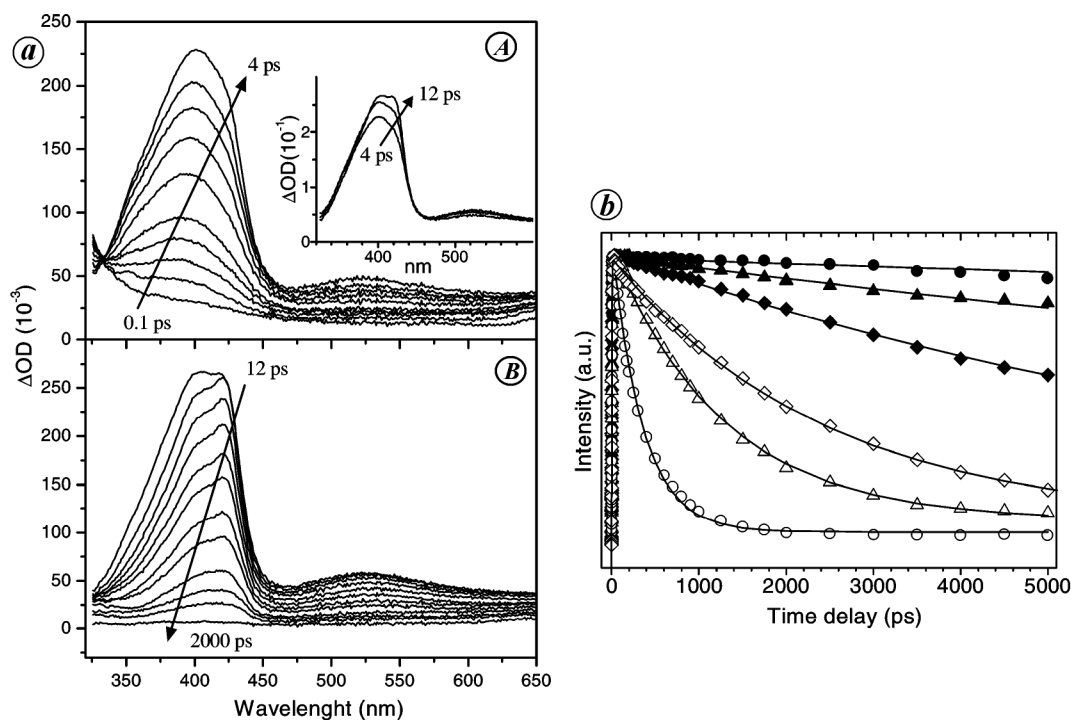


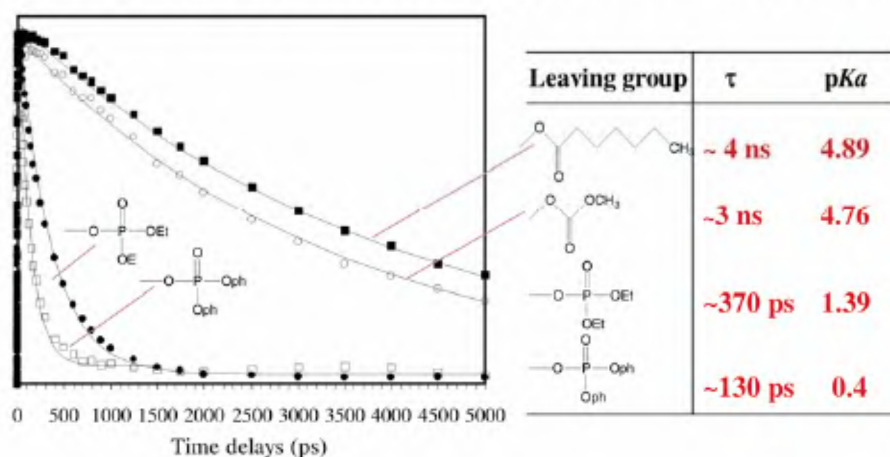
Figure 4. *a*, Transient absorption spectra of HPDP at early (*A*; from 0.1 to 12 ps) and late (*B*; from 12 to 2000 ps) picosecond times recorded with 267 nm excitation in H₂O/MeCN (1 : 1) mixed solvent. The right-hand part in (*A*) shows profile change of the transient absorption spectra recorded over 4–12 ps. *b*, Triplet decay kinetics observed for HPDP by transient absorption measurements in water/MeCN mixed solvent with water concentration of 0% (filled circles), 10% (filled diamonds), 15% (open diamonds), 25% (open triangles) and 50% (open circles). Data labelled by the filled triangles are obtained in a DMSO/CF₃CH₂OH (1 : 1 by volume) mixed solvent. Solid lines indicate dynamic fittings using a one exponential decay function to the experimental datapoints. (Reprinted with permission from ref. 12. Copyright (2006) American Chemical Society.)

the concerted triplet solvation and associated deprotection reaction. The importance of the leaving-group solvation is consistent and corroborated with results that show the triplet decay dynamics for the *p*HP compounds investigated (HPPP, HPDP¹¹ and HPA¹¹) is highly leaving-group-dependent, with the decay rate correlating with the stability of leaving-group anion (Figure 5). The observation that the ability of a good leaving group to stabilize the corresponding solvent solvated anion leads to an inducement of the photo-induced dissociation is characteristic of an excited-state heterolytic cleavage reaction²¹. The observed solvent and leaving group-dependent nature of the triplet decay dynamics provides strong evidence for a triplet-quenching process leading to direct heterolytic cleavage assisted by water solvation of the leaving-group anion. The need for the leaving-group solvation for *p*HP photodeprotection also helps to explain the complete lack of reactivity for HPDP in MeCN^{8,9} and DMSO solvents, since these two solvents are highly dipolar but cannot act as H-bond donors so they are poor at solvating the departing group²¹. Water solvation of the phenolic proton is also required to interpret the previous observation that photolysis of MPDP (the *p*-methoxy counterpart of HPDP) in a H₂O/MeCN (1 : 1) solvent results in little, if any, deprotection products^{6,9}. Since the hydroxy and

methoxy groups have similar electronic effects on the intrinsic property of the triplet states^{20,21}, the absence of reactivity for MPDP argues against a primary step involving simply the C–O bond heterolysis in the HPDP triplet and indicates that the proton-donating function of the hydroxy moiety in the *p*HP triplet is linked to the different photochemical reactivity of MPDP from HPDP in the same water/MeCN mixed solvent.

ps-TR³ experiments were done to observe the formation dynamics of the rearrangement product HPAA for photoexcited HPDP and HPPP in a H₂O/MeCN (1 : 1) mixed solvent. The UV absorption spectrum of HPAA shown in Figure 6*a* reveals that its lowest two absorption bands are weak, but HPAA absorbs strongly around 190–200 nm and therefore a 200 nm probe wavelength was selected for the ps-TR³ experiments. Figure 6*b* shows representative ps-TR³ spectra of HPDP at various delay times acquired with 267 nm pump and 200 nm probe wavelengths in a H₂O/MeCN (1 : 1) solution. The resonance Raman spectrum from an authentic sample of HPAA acquired under the same conditions and using a 200 nm excitation wavelength is also shown in Figure 6*b* to compare with and help identify the transient species seen in the TR³ spectra. The TR³ spectra display simultaneously the growth of a series of new Raman bands at

Leaving group dependence of the triplet quenching dynamics



✓ Correlation of the triplet quenching rate to the pK_a value of the leaving group anion suggests a direct triplet heterolytic cleavage mechanism

Figure 5. (Left) Temporal dependence of the transient absorption intensity for the triplet states of HPPP, HPDP, HPA and HPH in $H_2O/MeCN$ (1 : 1) at ~ 400 nm. Solid lines indicate kinetics fitting using a one exponential function to fit the experimental datapoints. (Right) The pK_a of the different leaving groups and time constants for the lifetime of the triplet states of HPPP, HPDP, HPA and HPH in $H_2O/MeCN$ (1 : 1) from the data shown in the left part of the figure. See text for more details.

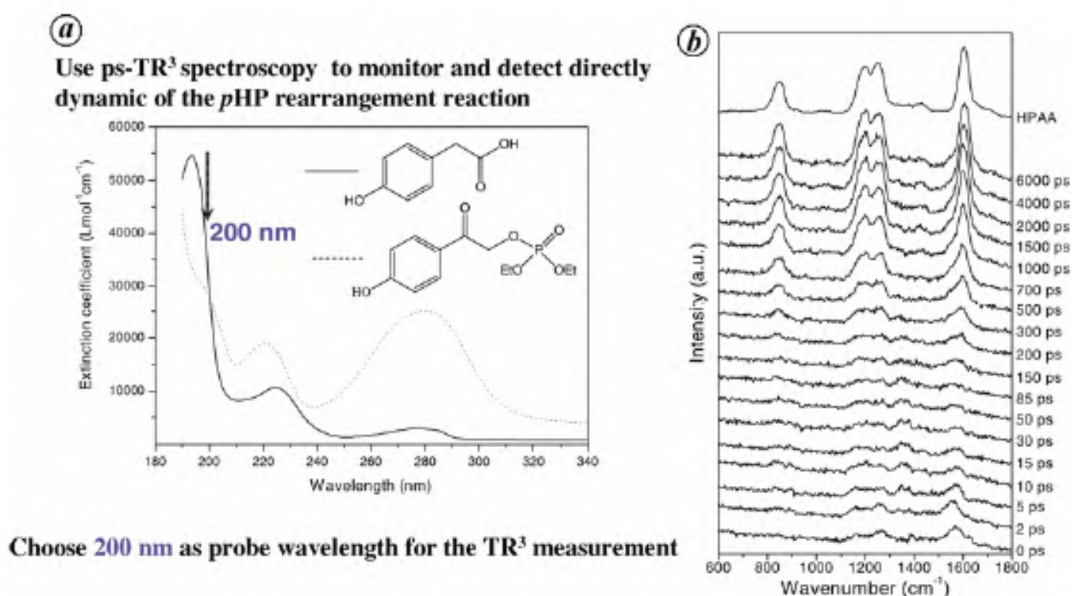


Figure 6. *a*, UV-VIS absorption spectra of the HPA product (solid line) and the HPDP substrate (dashed line) in a $H_2O/MeCN$ (1 : 1) mixed solvent. *b*, Picosecond time-resolved resonance Raman spectra of HPDP obtained with a 267 nm pump and a 200 nm probe wavelengths in a $H_2O/MeCN$ (1 : 1) mixed solvent. Resonance Raman spectra of an authentic sample of HPA recorded with 200 nm excitation is displayed in the top spectrum that is labeled with HPA. (Reprinted in part with permission from ref. 12. Copyright (2006) American Chemical Society.)

later picosecond times (~ 200 ps and afterwards) that are due to the production of a new species in this timescale. It is obvious that the new transient spectra are essentially identical to the 200 nm resonance Raman spectrum of an authentic sample of HPA. This clearly demonstrates

explicitly that the new species can be assigned unambiguously to the HPA rearrangement product. The data shown in Figure 6 *b* are a real-time monitoring of the dynamics for transformation from the photoexcited HPDP to the HPA final product and are to our knowledge, the

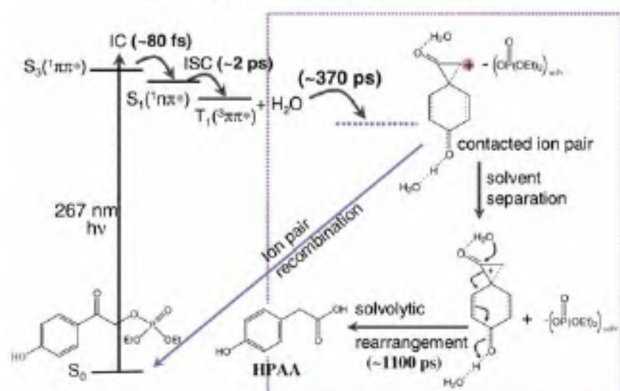
Solvent assisted triplet cleavage and stepwise solvolysis rearrangement reaction pathway for HPDP in H₂O containing solvent

Figure 7. Proposed overall mechanism for the deprotection and rearrangement reactions after ultraviolet photolysis of *p*HP phototrigger compounds based on the results of time-resolved spectroscopy experiments presented here. See text for more details.

first direct time-resolved detection of the solvolytic rearrangement reaction for *p*HP phototrigger compounds. A rough fit of these data in Figure 6 *b* by a one exponential growth function gives a time constant of ~1100 ps. Comparison with the ~350 ps time constant triplet decay time observed for HPDP in the same solvent indicates clearly that the rearrangement reaction is actually delayed relative to the triplet quenching process. Since the triplet decay time can be taken as the time constant for the release of the phosphate-leaving group, the delayed rearrangement dynamics indicates a consecutive reaction mechanism and the existence of an additional intermediate which is the direct product of the triplet deprotection and is the immediate precursor to the rearrangement process.

Based on the time-resolved spectroscopy results presented here, we can elucidate the basic reaction mechanism for the photodeprotection reaction that releases the phosphate-leaving group and the rearrangement reaction that forms the HPAA side product following photolysis of *p*HP phototriggers. This proposed mechanism is shown in Figure 7. A 267 nm photoexcitation of the *p*HP phototrigger compound takes it from its ground state to the $S_3(1\pi\pi^*)$ state that gives rise to the very short-lived blue fluorescence observed in the fs-KTRF experiments. This state undergoes very fast internal conversion of the order of 80 fs to form the $S_1(1n\pi^*)$ state that gives rise to the very short-lived (~2 ps lifetime) red fluorescence observed in the fs-KTRF experiments. The $S_1(1n\pi^*)$ state then undergoes very fast ISC to the $T_1(3\pi\pi^*)$ state. This was directly observed in both the ps-TR³ (Figure 3) and fs-TA experiments (Figure 4 *a*). The solvent effects observed in the TA experiments (Figures 4 and 5) are consistent with a solvent-assisted triplet heterolytic cleavage pathway for the release of the phosphate-leaving group and indicate that the strong coupling of water takes

place as site-specific concerted solvation of the hydroxy proton and phosphate-leaving group anion through their respective intermolecular H-bonding with solvent water molecules. This promotes the photodeprotection reaction. Correlation of the dynamics of the deprotection (for HPDP in 50% H₂O/50% MeCN solution this occurs with a time constant of ~350 ps, as depicted indicated in Figure 7) and rearrangement reactions (for HPDP in 50% H₂O/50% MeCN solution this occurs with a time constant of ~1100 ps as depicted indicated in Figure 7) indicates that there is a consecutive mechanism with the rearrangement occurring subsequent to the deprotection and that there is an involvement of an intermediate between the two reactions. The observed dynamics dependence on the solvent and the leaving group suggests that the intermediate is a solvation complex with contact ion pair character, as depicted in Figure 7. The results here provide important kinetics and structural data that allow an overall mechanistic characterization for the photophysical and photochemical events occurring after photolysis of *p*HP caged phosphates in various solvent environments. This information will be useful in designing and developing *p*HP caged compounds and related species for use as phototriggers.

- Givens, R. S. and Kueper, L. W., Photochemistry of phosphate esters. *Chem. Rev.*, 1993, **93**, 55–66 and references therein.
- Rock, R. S. and Chan, S. I., Preparation of a water-soluble ‘cage’ based on 3',5'-dimethoxybenzoin. *J. Am. Chem. Soc.*, 1998, **120**, 10766–10767.
- Lee, K. and Falvey, D. E., Photochemically removable protecting groups based on covalently linked electron donor–acceptor systems. *J. Am. Chem. Soc.*, 2000, **122**, 9361–9366.
- Zou, K., Miller, W. T., Givens, R. S. and Bayley, H., Caged thiophosphotyrosine peptides. *Angew. Chem., Int. Ed. Engl.*, 2001, **40**, 3049–3051.
- Il'ichev, Y. V., Schworer, M. A. and Wirz, J., Photochemical reaction mechanisms of 2-nitrobenzyl compounds: methyl ethers and caged ATP. *J. Am. Chem. Soc.*, 2004, **126**, 4581–4595.
- Givens, R. S., Weber, J. F. W., Conrad II, P. G., Orosz, G., Donahue, S. L. and Thayer, S. A., New phototriggers 9: *p*-hydroxyphenacyl as a C-terminal photoremovable protecting group for oligopeptides. *J. Am. Chem. Soc.*, 2000, **122**, 2687–2697 and references therein.
- Specht, A., Ludwig, S., Peng, L. and Goeldner, M., *p*-Hydroxyphenacyl bromide as photoremoveable thiol label: a potential phototrigger for thiol-containing biomolecules. *Tetrahedron Lett.*, 2002, **6**, 8947–8950.
- Conrad II, P. G., Givens, R. S., Hellrung, B., Rajesh, C. S., Ramseier, M. and Wirz, J., *p*-Hydroxyphenacyl phototriggers: the reactive excited state of phosphate photorelease. *J. Am. Chem. Soc.*, 2000, **122**, 9346–9347.
- Zhang, K., Corrie, J. E. T., Munasinghe, V. R. N. and Wan, P., Mechanism of photosolvolytic rearrangement of *p*-hydroxyphenacyl esters: evidence for excited-state intramolecular proton transfer as the primary photochemical step. *J. Am. Chem. Soc.*, 1999, **121**, 5625–5632.
- Brousmiche, D. W. and Wan, P., Excited state (formal) intramolecular proton transfer (ESIPT) in *p*-hydroxyphenyl ketones mediated by water. *J. Photochem. Photobiol. A*, 2000, **130**, 113–118.

11. Ma, C., Kwok, W. M., Chan, W. S., Zuo, P., Kan, J. T. W., Toy, P. H. and Phillips, D. L., Ultrafast time-resolved study of photo-physical processes involved in the photodeprotection of *p*-hydroxyphenacyl caged phototrigger compounds. *J. Am. Chem. Soc.*, 2005, **127**, 1463–1472.
12. Ma, C., Kwok, W. M., Chan, W. S., Du, Y., Kan, J. T. W., Toy, P. H. and Phillips, D. L., Ultrafast time-resolved transient absorption and resonance Raman spectroscopy study of the photodeprotection and rearrangement reaction of *p*-hydroxyphenacyl caged diethyl phosphate. *J. Am. Chem. Soc.*, 2006, **128**, 2558–2570.
13. Chan, W. S., Ma, C., Kwok, W. M. and Phillips, D. L., Time-resolved resonance Raman and density functional theory study of hydrogen-bonding effects on the triplet state of *p*-methoxyacetophenone. *J. Phys. Chem. A*, 2005, **109**, 3454–3469.
14. Zuo, P., Ma, C., Kwok, W. M., Chan, W. S. and Phillips, D. L., Time-resolved resonance Raman and density functional theory study of the deprotonation reaction of the triplet state of *p*-hydroxyacetophenone in aqueous solution. *J. Org. Chem.*, 2005, **70**, 8661–8675.
15. Chan, P. Y., Kwok, W. M. and Phillips, D. L., Time-resolved resonance Raman observation of the 2-fluorenylnitrenium ion reaction with guanosine to form a C8 intermediate. *J. Am. Chem. Soc.*, 2005, **127**, 8246–8247.
16. Givens, R. S., Matuszewski, B., Athey, P. S. and Stoner, M. R., Photochemistry of phosphate esters: an efficient method for the generation of electrophiles. *J. Am. Chem. Soc.*, 1990, **112**, 6016–6021.
17. Ramseier, M., Senn, P. and Wirz, J., Photohydration of benzophenone in aqueous acid. *J. Phys. Chem. A*, 2003, **107**, 3305–3315.
18. Banerjee, A. and Falvey, D. E., Direct photolysis of phenacyl protecting groups studied by laser flash photolysis: an excited state hydrogen atom abstraction pathway leads to formation of carboxylic acids and acetophenone. *J. Am. Chem. Soc.*, 1998, **120**, 2965–2966.
19. Ma, C., Zuo, P., Kwok, W. M., Chan, W. S., Kan, J. T. W., Toy, P. H. and Phillips, D. L., Time-resolved resonance Raman study of the triplet state of the *p*-hydroxyacetophenone and *p*-hydroxyphenacyl diethyl phosphate phototrigger compound. *J. Org. Chem.*, 2004, **69**, 6641–6657.
20. Ma, C., Chan, W. S., Kwok, W. M., Zuo, P. and Phillips, D. L., Time-resolved resonance Raman study of the triplet state of the *p*-hydroxyphenacyl acetate model phototrigger compound. *J. Phys. Chem. B*, 2004, **108**, 9264–9276.
21. Reichardt, C., *Solvent and Solvent Effect in Organic Chemistry*, VCH Verlagsgesellschaft mbH, D-6940 Weinheim, 1988.